Sixth International Symposium on Turbulence and Shear Flow Phenomena
Seoul, Korea, 22-24 June 2009

DNS OF VIBRATING GRID TURBULENCE

George Khujadze, Martin Oberlack
Chair of Fluid Dynamics,
Department of Mechanical Engineering,
Technische Universität Darmstadt,
Hochschulstr.1, 62489
Darmstadt, Germany
khujadze@fdy.tu-darmstadt.de
oberlack@fdy.tu-darmstadt.de

ABSTRACT

Results of direct numerical simulations (DNS) of vibrating grid turbulence are presented. Turbulence is generated at a grid in the $x_1 - x_2$ plane which vibrates normally to itself. There is no mean velocity in the flow. Hence, in a statistical sense turbulence is generated in a plane and diffuses out while at the same time gets damped due to dissipation. Due to zero mean shear there is no production of turbulence apart from the region at grid. Numerical simulations for two different Reynolds numbers (based on an amplitude and frequency of the grid) $Re = 500, 1000$ were performed using a spectral code. Statistics of turbulence was accumulated and the evolution of the turbulent/non-turbulent interface was detected and compared to the theoretical result obtained by Oberlack and Guenther (2003) using Lie group analysis. Good agreement was found between DNS and theoretical results.

INTRODUCTION

We consider the problem of free-shear turbulent diffusion with no production due to a mean-velocity gradient. Turbulence is generated at the plane $x_1 - x_2$ and diffuses in the direction $x_3 > 0$ (schematic view of simulation box is shown in the Fig. 1. In the middle of the box one can see the grid). Turbulence is homogeneous in the plane perpendicular to

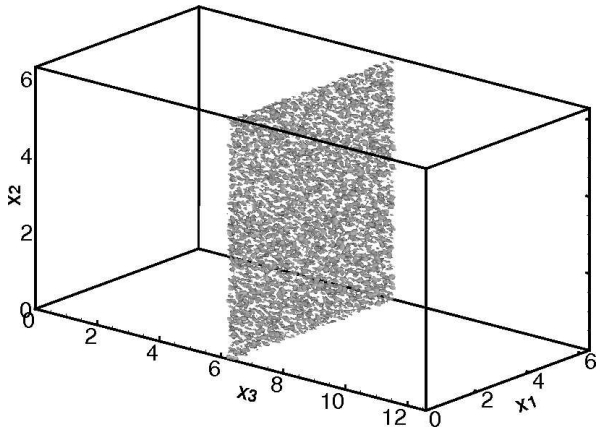

Figure 1: Schematic of the computational domain with the grid in the middle.

the diffusion. Experimentally, this problem is investigated by a plane vibrating grid in a sufficiently large tank. Grid is vibrating at a sufficiently small amplitude but at a large frequency. In the papers Hopfinger and Toly (1976), Hopfinger and Browand (1982) and De Silva and Fernando (1994) the results of a such experiments were reported. Vibrating grid in a water tank generates flow as a result of interactions between the individual jets and wakes created by the motion of the grid bars. Ideally no mean flow exists and turbulence is considered isotropic and homogeneous in planes parallel to the grid. Based on dimensional analysis Long (1978) predicted that the mean depth of the turbulent/non-turbulent interface $H(t)$ grows in time according to a power law $H(t) \sim t^{1/2}$. This was confirmed experimentally by Dickinson and Long (1978). Recently, Holzner *et al.* (2006) used detailed measurements and detection algorithm for the turbulent/non-turbulent interface and they confirmed the same propagation law. Even more recently in the group of Prof. Tropea from Technische Universität Darmstadt, Germany, the similar experiments were performed to study the rotating grid turbulence (see the paper by Kinzel *et al.* (2008) for details). They use the oscillating grid to generate turbulence in a water tank and PIV to determine the two-dimensional velocity and vorticity fields. They estimate the exponent of the power law and obtained the following expression:

$$H(t) \sim t^{0.5 \pm 0.1}.$$

Yang (1992) and Godeferd and Lollini (1999) performed numerical simulations in a context close to the experiments reported in the paper Hopfinger and Browand (1982). Yang (1992) used a pseudo-spectral code with two homogeneous directions along which the assumption that the flow is periodic. In order to model oscillating grid he introduced a complicated local forcing aimed to generate isotropic turbulence. This work dramatically suffered from the coarse vertical resolution. The next DNS was performed by Godeferd and Lollini (1999) with the similar pseudo-spectral code. They introduced a local forcing on a plane in physical space to simulate the effect of vibrating grid. In their simulations they achieved the Reynolds number $Re = 100$ at the grid.

PHYSICAL PROBLEM AND NUMERICAL METHOD

The main aim of this work was to the simulate turbulence generated by the vibrating grid similar to the experiments discussed in the introduction. For this purpose we numerically solve the incompressible Navier-Stokes equations:

$$\partial_i u_i = 0, \tag{1}$$

$$\partial_t u_i + \partial_j (u_i u_j) = -\frac{1}{\rho}\partial_i p + \nu \nabla^2 u_i, \tag{2}$$

within a parallelepiped domain with dimension $L_1 = L_2 = 2\pi$, $L_3 = 2\pi \cdot d$ (where d is an integer number) and with the periodicity conditions in all directions:

$$u_i(\mathbf{x} + L_j \mathbf{e}_j, t) = u_i(\mathbf{x}, t), \quad i = 1, 2, 3. \tag{3}$$

These boundary conditions are suited to simulate homogeneous and isotropic turbulent fields. The mathematical structure of the problem leads naturally to the adoption of a spectral discretization and in particular to a Fourier-Galerkin method. To keep the advantage of the spectral method, we locate the grid in the middle of the simulation box that allows us to use periodic boundary conditions and apply Fourier decomposition in all three directions. Fourier-Galerkin spatial discretisation method was coupled with a low storage fourth order Runge-Kutta scheme for the time integration (for details see Iovieno *et al.* (2006)).

To mimic the action of the grid the function introduced in the work by Godeferd and Lollini (1999) was used in our simulations with small modifications. We implemented a local forcing on a plane in the physical space simulating the effect of an oscillating grid, so that diffusive turbulence is created. The external force $f_i(x_1, x_2)$ has the following form (Fig. 2):

$$f_i = \frac{n^2 S}{2}\left\{\left|\frac{\delta_{i3}}{4}\cos\left(\frac{2\pi}{M}x_1\right)\cos\left(\frac{2\pi}{M}x_2\right)\right|\sin(nt)+\frac{\beta_i}{4}\right\}, \tag{4}$$

where M is the mesh size, $S/2$ – amplitude (stroke of the grid), n – frequency. β_i are random numbers with the uniform distribution. The chosen shape of the forcing is a superposition of a deterministic function that explicitly contains the grid parameters (mesh size, amplitude and time frequency) and of a random component. Turbulence generated by such a forcing is similar to that one generated by an oscillating grid in experiments. Our forcing (4) is different from that one introduced in the paper by Godeferd and Lollini (1999) where alternating sources and sinks were introduced. We have modified the grid function to get results analogous to the experiments by Kinzel *et al.* (2008). In their experiments turbulence propagates away from the grid and dissipates, being a result of interactions between the individual jets and wakes created by the motion of the grid bars.

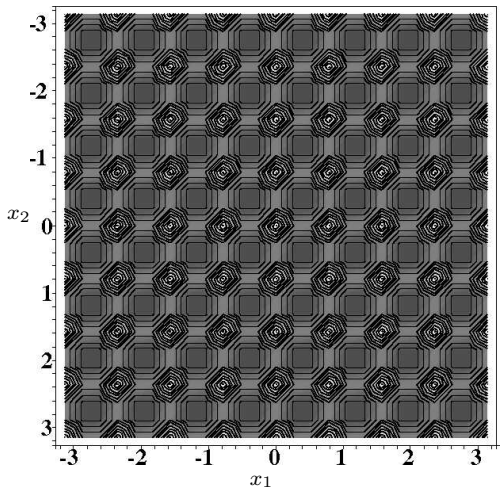

Figure 2: Schematic view of the grid function without the random part.

All the following quantities presented are non-dimensionalized with the help of the reference length S and time frequency n. Choosing S and n as the reference length and time frequency scales, we can define Reynolds number in the following manner:

$$Re = \frac{nS^2}{\nu}. \tag{5}$$

The simulations are performed using a numerical domain of the size: $x_1, x_2 \in [-\pi;\pi], x_3 \in [-2\pi;2\pi]$. The Reynolds numbers, ratio of the grid amplitude to the mesh size and the number of modes have the following values in the performed DNS:

$$\begin{gathered} Re = 500, 1000; \quad \frac{S}{M} = 2; \\ N_x \times N_y \times N_z = 128\times128\times128; \quad 128\times128\times256. \end{gathered} \tag{6}$$

The number of "rods" in the grid was 32. We performed the DNS at the two different Reynolds numbers given above with a mesh size twice as small as the grid stroke. This ratio was also chosen in the experiment by Kinzel *et al.* (2008). The Reynolds number achieved in the paper Godeferd and Lollini (1999) was $Re = 20$ that is much smaller than that one achieved in the experiments where it was of the order of 3000. Our aim was to perform a DNS with the Reynolds number closer to the experimental one. The presented DNS results are obtained at Reynolds numbers much higher than reported in the paper Godeferd and Lollini (1999) but still smaller than in the experiments. However, the results show good agreement to the theory (Oberlack and Guenther, 2003) and experiments (Kinzel *et al.*, 2008).

RESULTS OF NUMERICAL SIMULATIONS

First we show the behavior of turbulent kinetic energies. Figs. 3 and 4 exhibit the turbulent kinetic energy normalized on the energy at the grid vs. x_3 for low ($Re = 500$) and high ($Re = 1000$) Reynolds number cases at the different time snap shots. We see that the kinetic energy dissipation is faster in the case of high Reynolds number case as it was expected. Next two figures (Figs. 5 and 6) represent

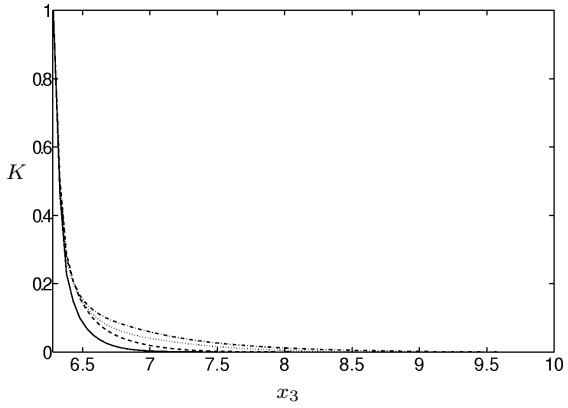

Figure 3: Normalized turbulent kinetic energy ($K/K|_{grid}$) at $Re = 500$: —— $t = 100$, – – – $t = 200$, ····· $t = 400$, —·— $t = 600$.

the turbulent kinetic energy (non-normalized and normalized correspondingly) comparison for the different Reynolds numbers. Dashed line corresponds to $Re = 500$, solid line shows $Re = 1000$.

In the paper of Oberlack and Guenther (2003) authors using Lie groups analysis of the multi-point correlation equations consider the problem of shear-free turbulent diffusion. They obtained three different invariant solutions or scaling

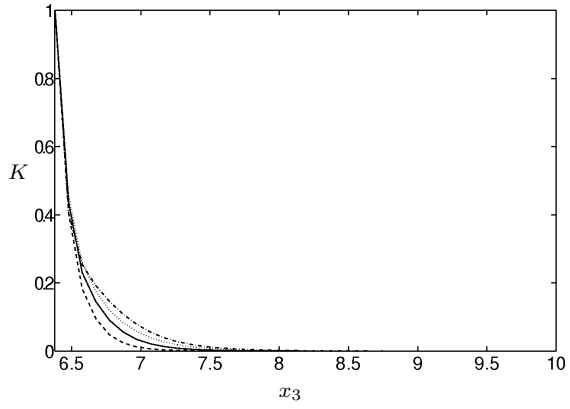

Figure 4: Normalized turbulent kinetic energy at different Reynolds numbers $Re = 1000$: − − − $t = 100$, —— $t = 200$, ····· $t = 400$, —·— $t = 600$.

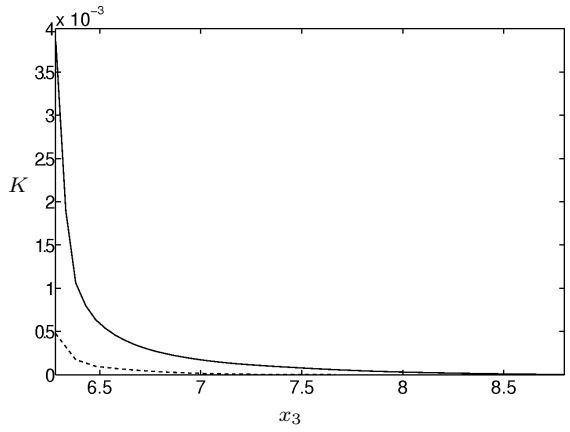

Figure 5: Non-normalized turbulent kinetic energy at different Reynolds numbers − − − $Re = 500$, —— $Re = 1000$.

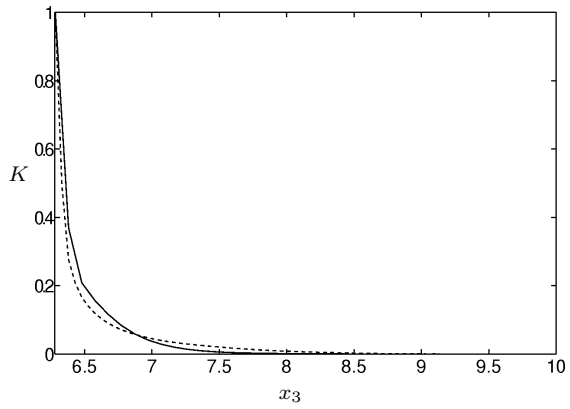

Figure 6: Normalized turbulent kinetic energy at different Reynolds numbers − − − $Re = 500$, —— $Re = 1000$.

laws: classical diffusion-like solution, deccelerating diffusion-wave solution and finite domain diffusion due to rotation. In our study we considered only the first case. One of the main results of the paper Oberlack and Guenther (2003) was that the mean depth the of the turbulent/non-turbulent interface evolves in time by the following power law:

$$H(t) = A(t - t_0)^m + B, \qquad (7)$$

where A, m, B are constants. One of the main aim of our DNS was to validate this power law and find the values of the constants. Figs. 7 and 8 show the mean depth of the

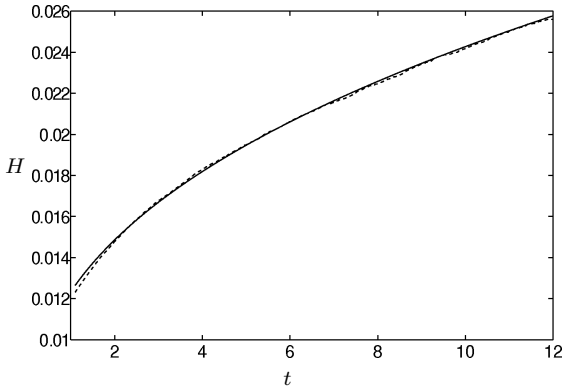

Figure 7: Mean position of the turbulence/non-turbulence interface $H(t)$ in linear axes. —— theoretical result and − − − DNS.

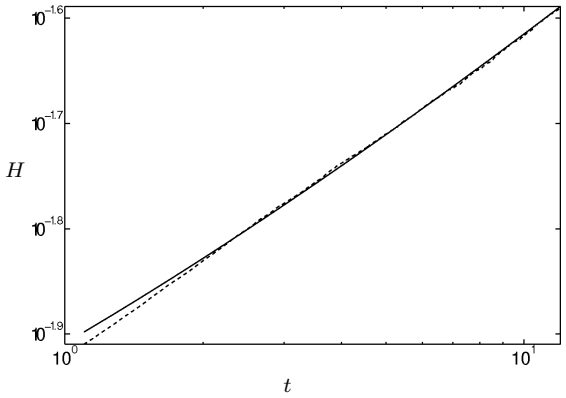

Figure 8: Mean position of the turbulence/non-turbulence interface $H(t)$ in logarithmic axes. —— theoretical result and − − − DNS.

turbulent/non-turbulent interface $H(t)$ in linear and logarithmic scaling correspondingly. Constants in equation (7) taken from the DNS have the following values in our normalizations: $A = 1.7\ 10^{-3}$; $B = 0.5\ 10^{-2}$; $t_0 = 0$; $m = 0.4$. The value of m is close to the experiments performed by Kinzel *et al.* (2008) where it was obtained that $m = 0.5 \pm 0.1$. As one can see from the Figs. 7 and 8 there is good agreement between DNS and theory. Curves representing the DNS and theoretical results (dashed line for DNS and solid one for the theoretical result) collapse in one.

As for the turbulence structure itself plots in Fig. 9 shows velocity fields for different moments of simulation time: $t = 0$; 20; 50 at small Reynolds number case. As it is observed from the figure, at $t = 0$ the turbulence structures are comparable to the mesh size, but as DNS evolves the length scales grow in the direction $x_3 > 0$.

Fig. 10 represents the time evolution of kurtosis (see equation 8) at $Re = 500$. As we see from the figure the peak of the kurtosis increases in time. The high peak means that the turbulence at lower Reynolds number is far from a homogeneouty. This is clearly seen from the velocity fields presented in Fig. 9. The turbulent structures increase away

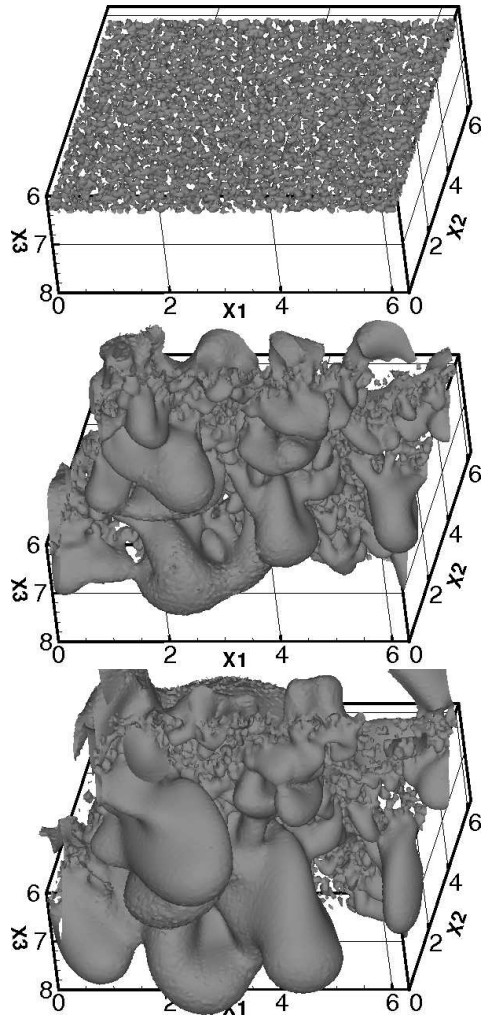

Figure 9: Velocity fields for different snapshots $t = 0; 20;\ 50$ at $Re = 500$.

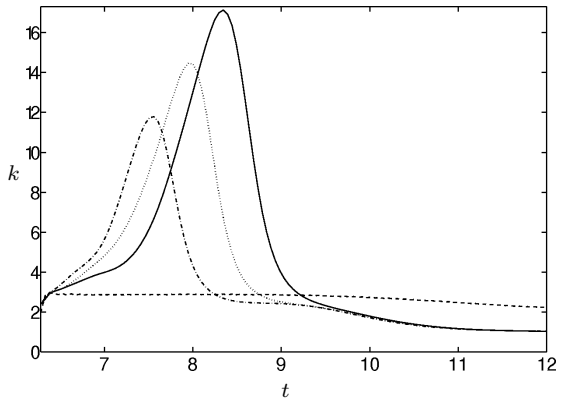

Figure 10: Time evolution of kurtosis at $Re = 500$. – – – $t = 0$; —·— $t = 25$; ····· $t = 50$; —— $t = 100$.

from the grid.

$$k = \frac{\overline{u}^4}{(\overline{u}^2)^2}. \tag{8}$$

Fig. 11 shows the instantaneous velocity field at $t = 0;\ 20;\ 50$ for $Re = 1000$. In this case the turbulent field is closer to homogeneouty which is also confirmed by the comparison of kurtosis presented in the Fig. 12. This figure

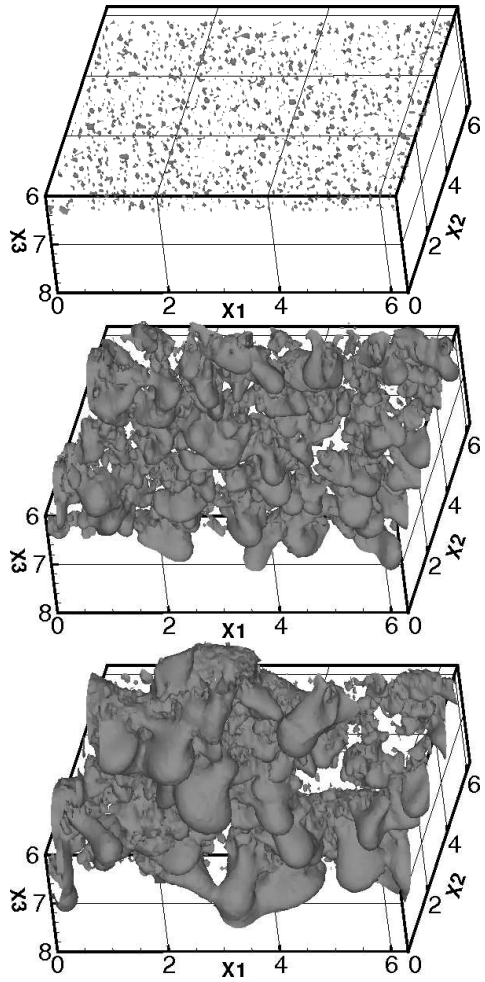

Figure 11: Velocity fields for different snapshots $t = 0;\ 40;\ 60$ at $Re = 1000$.

shows the kurtosis at $Re = 500$ (solid line) and $Re = 1000$ (dashed line).

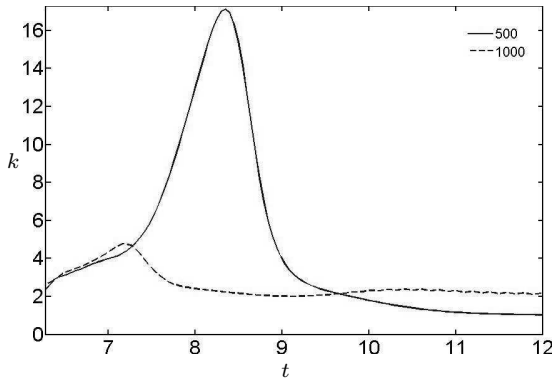

Figure 12: Comparison of Kurtosis at $Re = 500$ (—— line) and $Re = 1000$ (– – – line).

Figs. 13 and 14 show the r.m.s. components of velocity. Horizontal/non-homogeneous u_h and vertical/homogeneous u_v components of r.m.s we define as it follows:

$$u_h = \sqrt{\overline{u_3^2}},$$

$$u_v = \frac{1}{2}(\sqrt{\overline{u_1^2}} + \sqrt{\overline{u_2^2}}).$$

As one can see the horizontal/non-nhomogeneous compo-

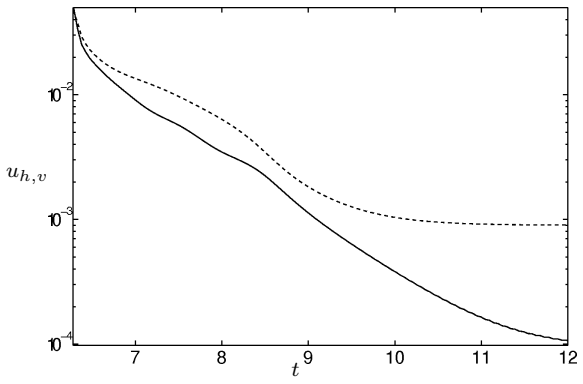

Figure 13: Spatial evolution of the r.m.s. velocity components at $Re = 500$. – – – u_h, —— u_v.

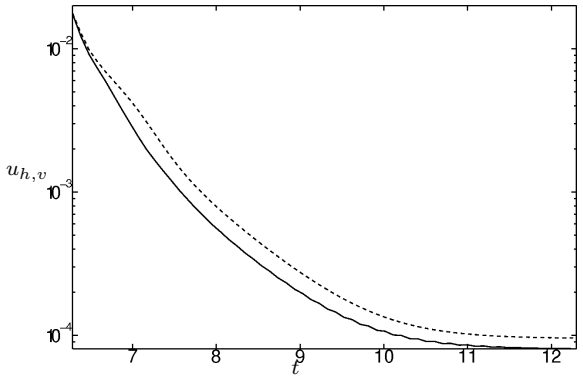

Figure 14: Spatial evolution of the r.m.s. velocity components at $Re = 1000$. – – – u_h, —— u_v..

nent of r.m.s in the case of high Reynolds number case decreases by the same law as the vertical/homogeneous component does. It means that in this case the turbulence is homogeneous as it was shown from the figures of velocity fields (see Fig. 11). As for the low Reynolds number case, the bahavior of the horizontal component of r.m.s is different than the behavior of the vertical one. In this case the turbulence is not homogeneous in the horizontal (the direction perpendicular to the grid plane) direction that was also shown by the instantaneous velocity fields (see Fig. 9).

CONCLUSION

DNS of grid turbulence was performed for two different Reynolds numbers $Re = 500,\ 1000$. The power law of time evolution of the turbulent/non-turbulent interface H was validated and good agreement was found between DNS and theoretical results. The value of the power constant was found close to the experimental one. Statistics of the grid turbulence was accumulated for long simulation time and presented in the paper. Instantaneous turbulent structures were compared for different Reynolds numbers.

ACKNOWLEDGEMENTS

Authors thank to Dr. M. Iovieno and Prof. D. Tordella from Politecnico di Torino, Italy for their help in the development of the code. G.Kh. thanks them for their hospitality during his visits in Torino.

*

REFERENCES

De Silva, I. and Fernando, H. (1994). Oscillating grids as a source of nearly isotrpoic turbulence. *Phys. Fluids*, **6**(7), 2455–2464.

Dickinson, S. and Long, R. (1978). Laboratory study of the growth of a turbulent layer of fluid. *Phys. Fluids*, **21**(10), 1698–1701.

Godeferd, F. and Lollini, L. (1999). Direct numerical simulations of turbulence with confinement and rotation. *J. Fluid Mech.*, **393**, 257–308.

Holzner, M., Liberzon, A., Guala, M., Tsinober, A., and Kinzelbach, W. (2006). Generalized detection of the turbulent front generated by an oscillation grid. *Exp. In Fluids*, **41**(5), 711–719.

Hopfinger, E. and Browand, F. (1982). Turbulence and waves in a rotating tank. *J. Fluid Mech.*, **125**, 505–534.

Hopfinger, E. and Toly, J. (1976). Spatially decaying turbulence and its relation to mixing across density surfaces. *J. Fluid Mech.*, **78**, 155–177.

Iovieno, M., Cavazzoni, C., and Tordella, D. (2006). A new technique for a parallel dealiased pseudespectral navier-stokes code. *Computer Physics Communications*, **141**, 365–374.

Kinzel, M., Holzner, M., Lüthi, B., Tropea, C., Kinzelbach, W., and Oberlack, M. (2008). Scaling laws of turbulent diffusion – an experimental validation. 14th Int Symp on Applications of Laser Techniques to Fluid Mechanics, Lisbon, Portugal.

Long, R. (1978). Theory of turbulence in a homogeneous fluid induced by an oscillating grid. *Phys. Fluids*, **21**(10), 1887–1888.

Oberlack, M. and Guenther, S. (2003). Shear-free turbulent diffusion – classical and new scaling laws. *Fluid Dynamics Research*, **33**, 453–476.

Yang, G. (1992). *DNS of boundary forced turbulent flow in a non-rotating aand rotating system*. Ph.D. thesis, Cornell University.